Application of HSPF to the Distributed Model Intercomparison Project: Case Study

Jae H. Ryu[1]

Abstract: The Hydrologic Simulation Program–Fortran (HSPF) model was used to simulate streamflow for the Distributed Model Intercomparison Project (DMIP). This research describes how to integrate a next generation radar, NEXRAD data set into HSPF model and how to generate hydrologic runoff associated with the inputs of the spatial rainfalls, and discusses the challenges of HSPF during automatic calibration processes. The model performance of simulated streamflows with calibration and without calibration was also evaluated to assess the sensitivity of final estimated parameters through calibration procedures to initial parameters derived from physical watershed configuration. An automatic calibration scheme was adopted to optimize objectives that the writer specified in terms of statistical measures. Parameter estimation, a model-independent parameter estimator, was used as an automatic calibration tool in the hydrologic calibration of HSPF. Overall, the calibrated simulations outperformed the uncalibrated simulations for DMIP basins, and the writer anticipates that HSPF may be a potential alternative model to reproduce the hourly flows for streamflow forecasts.

DOI: 10.1061/(ASCE)HE.1943-5584.0000054

CE Database subject headings: Hydrologic models; Rainfall; Runoff; Streamflow; Forecasting; Case reports.

Introduction

Hydrologic models are evolving to incorporate high-resolution data, high-performance computation, and complex geophysical modeling frameworks. Since the 1960s, many rainfall-runoff models have been widely applied to many different watersheds, nationally and internationally. However, it appears that such models would have difficulty integrating a high resolution of spatial variability of precipitation into hydrologic simulations not only because the modeling structures and limited parameterization are challenging but also because modern rainfall-runoff models have not been designed with the intent to interface with high-resolution (in space and time) input data products. Many studies have been conducted to analyze the sensitivity of streamflow realizations associated with spatial variability of forcing data, and these studies have showed that spatial distribution of rainfall would be the dominant factor in simulating streamflow hydrographs as opposed to point observation data (Ogden and Julien 1994; Shah et al. 1996a,b; Wilson et al. 1979). It is also noted that spatially distributed rainfall data diminish the bias between observed and simulated hydrographs because of the smoothing of errors embedded in finer data resolutions (Koren et al. 1999). Such findings encouraged many hydrologists to migrate to a distributed hydrologic model and a semidistributed model as a basis of a lumped hydrologic model. Moreover, recent radar technology has facilitated applications of spatial and temporal variability of precipitation to simulate and improve runoff hydrographs.

In January 2000, the Hydrology Laboratory (HL) of the National Oceanic and Atmospheric Administration/National Weather Service (NOAA/NWS) initiated the Distributed Model Intercomparison Project (DMIP) to improve river and streamflow forecasts associated with modeling systems based on next generation radar (NEXRAD) multisensor precipitation products. Results of the first phase (2000–2002) of DMIP (DMIP1) suggest that the spatial rainfall derived from NEXRAD can improve streamflow forecasts in higher-order stream-embedded basins (Smith et al. 2004). This phase also provided a significant emphasis on the hydrologic modeling framework and compared the performances between existing distributed models and lumped models in terms of model formulation, parameterization, and levels of calibration (Reed et al. 2004).

Although the hydrology community has had numerous discussions about comparisons between distributed models versus lumped models, they have not been able to determine which type of model has a better overall performance. For instance, Boyle et al. (2001) found that significant performance improvement of the distributed model over the lumped model was provided by the spatial variability of the rainfall and modeling components, such as soil moisture and streamflow routing computation, while Bell and Moore (1998) suggest that a well-constructed lumped model is preferred for routine operational flood forecasting in the study area in the United Kingdom. Additionally, Michaud and Sorooshian (1994) compared a lumped and a distributed model for simulations of 24 severe storm events, and the results showed that the lumped model performed poorly when calibration is not performed. Similarly, Refsgaard and Knudsen (1996) have conducted a case study on validation and intercomparison of lumped and distributed models on three catchments in Zimbabwe, and they agreed that the distributed models performed marginally better for cases where no calibration was allowed.

More recently, Reed et al. (2004) extended this theme by the DMIP results that the lumped model performed better than distributed models, but some distributed models also showed comparable results to lumped models in many basins. The interested reader is referred to Smith et al. (2004) and many other related

[1]Hydrologist, School of Natural Resources, Univ. of Nebraska, Lincoln, NE 68583-0988. E-mail: jryu2@unl.edu

Note. This manuscript was submitted on November 12, 2007; approved on November 17, 2008; published online on February 12, 2009. Discussion period open until January 1, 2010; separate discussions must be submitted for individual papers. This paper is part of the ***Journal of Hydrologic Engineering***, Vol. 14, No. 8, August 1, 2009. ©ASCE, ISSN 1084-0699/2009/8-847–857/$25.00.

publications for additional discussions about comparisons between distributed and lumped models. Particularly, Vieux et al. (2004) thoroughly represent the accomplished project in terms of many key procedures taken into account in hydrologic modeling, including theory, calibration parameters, and modeling concepts in the development of distributed models.

In light of key findings from DMIP1 as well as literature reviews, NOAA/NWS extended an intercomparison work to a second phase of DMIP (DMIP2) to identify more critical modeling issues associated with computational requirements in an operational environment and forecasting setting. Although participants are allowed to use any rainfall-runoff models, the selected models should meet a list of specific requirements of the NWS, such as the capability of distributed modeling, adoptability of high-resolution data sets (e.g., NEXRAD), the ability to generate simulations at ungauged streamflow simulations, and potential of streamflow forecasts. Based on experiences in DMIP1, NOAA/NWS has identified some real benefits of using the distributed models for the DMIP basins over the lumped models. For instance, although the lumped models show better performance than the distributed models in most cases, some distributed models outperformed lumped models after calibration at a level of current operational standard. Furthermore, clear gains in predicting peak flows from distributed models were noticeable in both midsized and small basins (Reed et al. 2004). These findings encouraged the participant to see distributed modeling as a key pathway to facilitate a new science agenda into river forecast operations and services.

In this study, the Hydrological Simulation Program–Fortran (HSPF) model system was selected not only because it is a rainfall-runoff model linking surface dynamics to groundwater recharges through climate forcing data, but also because it provides a wide range of flexibility for model formulation and calibration processes. No paper has been published dealing with streamflow simulations using HSPF with NEXRAD forcing in a high-resolution spatial (8 km by 8 km) and temporal (hourly) modeling environment required to meet the DMIP's modeling criteria discussed above.

The goal of this paper is to explore the potential use of HSPF as a real-time hydrologic forecasting tool for NWS with three objectives, including: (1) how to set up and run HSPF within a distributed modeling framework along with spatially distributed forcing data; (2) what the recurrent challenges during automatic calibration in HSPF are; and (3) what the differences of hydrologic performances between models associated with uncalibrated and calibrated parameters are. The following sections of this paper include descriptions of the model, methodology, and data used in this study. Next, detailed calibration procedures using an automatic calibration tool, the Parameter Estimation (PEST) software (which minimizes model biases formulated in user-specified objective function), are described. Results and conclusions of the DMIP experiment are given. The model's performance was evaluated initially over two characteristic periods, a calibration period (October 1, 1996–September 30, 2002) and a verification period (October 1, 2002–September 30, 2006), but note that most of the results are shown in calibration periods because no significant hydrologic behavior associated with the calibrated parameters of HSPF was identified in validation periods. The writer anticipates that automatic calibration of HSPF with PEST using radar rainfall data, calibrated hydrologic parameters, methodology, and the results of this study will contribute to the case for promoting a novel methodology or innovative application in hydrologic communities.

Model Description

HSPF is a rainfall-runoff model to simulate hydrologic runoff and water quality processes on pervious (e.g., forest, farmland) and impervious (e.g., urban area) land segments and river channels. The strength of the HSPF model is comprehensive modeling capabilities, including cell-based representation of land segments and drainage channels; subdivided storage columns to denote the water available for infiltration, runoff, and groundwater recharges; and automatic calibration tools to optimize model performance by adjusting hydrologic parameters (e.g., WinHSPF Version 2.3 build 8).

The basic routine of HSPF is simulating each subbasin depending on the specific watershed delineation. Each subbasin is simulated according to pervious land segment (forest, agricultural, and urban built-up), impervious land segment (urban built-up), and stream or mixed reservoir segment (RCHRES). HSPF employs several storage zones to represent the storage processes that interact and occur simultaneously on the land surface and in the soil columns. Precipitation moves to the upper-zone soil layer and overflow can be generated for infiltration to a lower-zone soil layer and runoff processes if the soil layer in the upper zone is fully saturated.

The RCHRES simulates the flow of water in the tributary that drains each basin. Flow through a RCHRES, which is a one-dimensional fluid dynamic model and complete mixing system, is assumed to be unidirectional and the RCHRES uses the kinematic method for channel routing. To generate a runoff hydrograph with the model, 1 year of existing meteorological data (October 1, 1995–September 30, 1996) just before the simulation is run through the model to capture the initial conditions. HSPF uses both conceptual and physical approaches to represent rainfall-runoff dynamics. Soil moisture storage concepts associated with water table conditions determine parameters such as storage capacities in the upper- and lower-zone soil layers, while runoff mechanics driven by rainfall through surface terrain influence physical parameters such as land slope, channel profile, Manning roughness, infiltration rate, and interception capacity of vegetation.

Study Area and Data

Study Area

Three river basins, the Illinois River, Elk River, and Blue River, were selected for DMIP2 not only because these basins had a data-rich environment (high-quality NEXRAD radar-based rainfall data are available in this region back to 1993), but also because there are no complications such as upstream diversions, dam operations, or snow. Additionally, the prediction of interior hydrologic processes inherited from parent basins can be easily developed for research questions in this study (Smith et al. 2004). Elk River Basin is located near the border between Missouri and Arkansas, and the drainage area of the basin is 2,258 km^3. The Illinois River Basin lies to the south of the Elk basin, starting drainage from the US Geological Survey (USGS) gauge at Osage Creek at Cave Springs, Ark. (AR), covering the Illinois River basin above Watts, Okla. and Savoy, Ark., and ending at the USGS gauge at Talequah, Okla. The total drainage area of this basin is 2,484 km^3, which is the largest basin in this study.

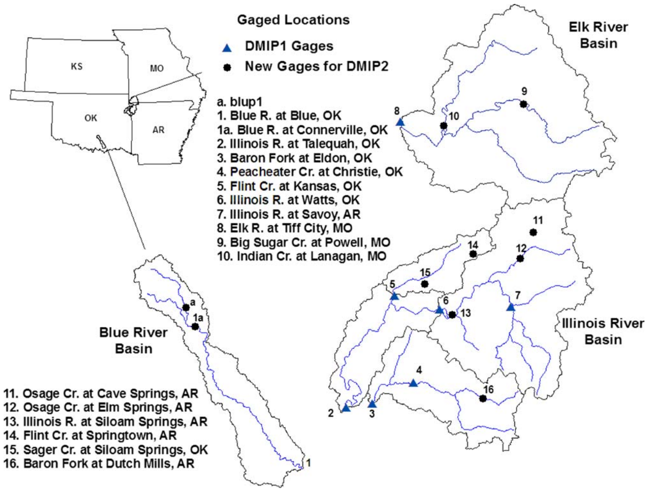

Fig. 1. Study area of DMIP2 basins. Note that triangles represent USGS stream gauges used for DMIP1 and circles indicate new gauges added for DMIP2.

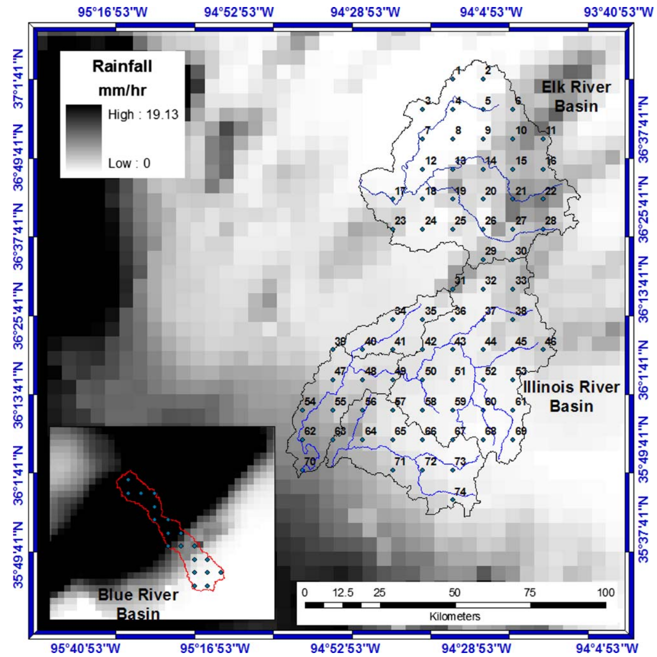

Fig. 2. Pseudoraingauge network location corresponding to NEXRAD rainfall product for Elk, Illinois, and Blue River Basins. Note that radar rainfall reflectivity (mm/h) is collected at 1:00 a.m., October 1, 1995, central standard time.

Blue River Basin is a relatively small basin and its total drainage area is 1,233 km^3. It lies to the south near the border with Texas (Fig. 1).

Precipitation

The NWS provided multisensory radar-based precipitation estimates that were developed by the River Forecast Center (RFC) as forcing data for hydrologic models. These data have been corrected based on a combination of radar estimates and their adjustment by local gauges of hourly rainfall accumulation on 4 km by 4 km resolution produced at the NWS River Forecast Center. The correction and adjustment of radar rainfall input is called the Process-1 (P1) method. The reader is referred to Fulton et al. (1998), Young et al. (2000), and Wang et al. (2000) for details on NEXRAD precipitation products, implementation, and data processing using algorithms, respectively. Hourly rainfall estimates are written in a binary format (e.g., xmrg) on a Hydrologic Rainfall Analysis Project (HRAP) grid generated by Stage III radar algorithms. As a basis of the polar stereographic projection, a HRAP grid system is used for precipitation estimations from WSR-88D radars (Greene and Hudlow 1982). To implement NEXRAD data into HSPF, the numbered pseudo-rain gauge network with 8 km by 8 km spatial resolution are created and located along the basins to capture the hourly NEXRAD rainfalls (Fig. 2). The finer spatial resolution (4 km by 4 km) is preferred for retrieving NEXRAD data for the HSPF model because of its original cell size of rainfall data, but 8 km by 8 km spatial resolution was utilized instead because such resolution is suitable for implementing the other forcing data, potential evapotranspiration (PE) from North American Regional Reanalysis (NARR) data (described in the next section). However, if the basin consists of highly mountainous areas where the adiabatic lapse rate changes rapidly over altitude or significantly different land use profiles and soil characteristics between specified cells, it is hypothesized that a distributed model with finer spatial resolution would provide performance gains over a lumped model.

Rainfall input to the hydrologic model components is given as function of subbasin mean areal precipitation (MAP) computed at each time step based on the radar rainfall estimates (Carpenter and Georgakakos 2004). Thus, rainfall in a resolution of 8 km by 8 km is averaged in subbasins, and then routed into HSPF as a forcing.

Potential Evapotranspiration

As previously described, no significant snow accumulation occurs in this particular basin, and only potential evapotranspiration and precipitation are required for hydrological runoff processes in the HSPF model. To calculate actual evapotranspiration in HSPF, potential evapotranspiration is used in subroutine group EVAP. Potential evapotranspiration data as a subset of the NARR data set is available from the National Centers for Environmental Prediction (NCEP) (Mesinger et al. 2004; Mitchell et al. 2004). Advantages of the NARR data set include its capability to better treat land surface dynamics through a land-surface model (NOAH) forced by observed precipitation and surface winds associated with vegetation type, soil profiles, and geopotential heights (Ek et al. 2003). To resolve spatial resolution between NEXRAD rainfall (8 km by 8 km) and NARR potential evapotranspiration (32 km by 32 km), each grid point is interpolated to the internal latitude/longitude grid cells using a grid decoder (e.g., GrADS). A temporal disaggregation is also conducted using a triangular distribution centered on the middle of the hour. Although the NARR-A data are available at 3 h, it is inconvenient to incorporate it directly into the hydrologic model, which requires an hourly time step. For this study, an hourly time step was used and recommended by NWS to analyze the model's performance in a short time step, which is able to identify the peaks during flash floods.

Digital Elevation and Stream Network

Two different resolutions of digital elevation model (DEM) files, 15 arcsec (0.0041666°, spatial resolution around 90 m) interval, which are resampled from 3 arcsec DEMs (1:250,000 scale), and 1 arcsec (7.5 min DEM, 30 m resolution) interval, are provided by NWS, but any DEM data such as the US Geological Survey (USGS) may be used by all participants. For topographic relief mapping, watershed delineations and modeling, and flow direction computing, 15 arcsec DEM (1:250,000 scale) are employed in this study. The initial coordinate system of the DEM refers to the geographic coordinate system (North American Datum of 1983) in decimal degrees, but it is reprojected to a designated coordinate projection system (State Plane Projection, Oklahoma, in this study). The Elk and Illinois River basins and the Blue River Basin are reprojected to north and south Oklahoma, respectively. The stream network can be generated based on the DEM or defined by an existing stream reach file (e.g., USEPA reach file). For modeling feasibility, the National Hydrography Dataset (NHD) is utilized to develop stream routing for hydrologic modeling because it is designed to incorporate a detailed stream network in high resolution (1:100,000 scale) required by many distributed hydrology models.

Land Use and Soil

As environmental background data, land use coverage and soil characteristics are prepared to perform a more detailed assessment of watershed conditions and hydrologic cycles. Land use coverage, a polygon shape in vector format that represents boundaries associated with land use classifications including Anderson Level 1 (urban or built-up land, agricultural land, forest land, water, and barren land) and Level 2 (Anderson et al. 1976), is available from the Geographic Information Retrieval and Analysis System (GIRAS) of USGS. Two different resolutions of soil data, the Soil Survey Geographic (SSURGO) database and State Soil Geographic (STATSGO) soil data [compiled and distributed by the Natural Resources Conservation Service (NRCS) of the U.S. Department of Agriculture], are available to DMIP participants. Since SSURGO data, however, are not scheduled to be completed until 2008, STATSGO soil data were utilized for this study instead (USDA 1994).

Methodology

Watershed Delineation

Automatic delineation is commonly used to delineate watersheds based on an automatic procedure associated with elevation (DEM), masking of the boundary focusing watershed area, and stream network (NHD). The initial stream network and subbasin outlets can be easily defined through stream definition processes by determining a minimum and maximum basin area with threshold. These functions are extremely important to determine the details of the stream network and the size and number of the created subbasins where observed streamflow data are available at interior points for "blind" simulations to evaluate performance of interior simulation when calibration was made at the basin outlet. A total of 17 outlet points (two from Elk, 12 from Illinois, and three from Blue) are added into the delineated watershed to generate hydrographs at the specified locations, including the blup location shown as "blup1" in Fig. 1. Note that the area studied is

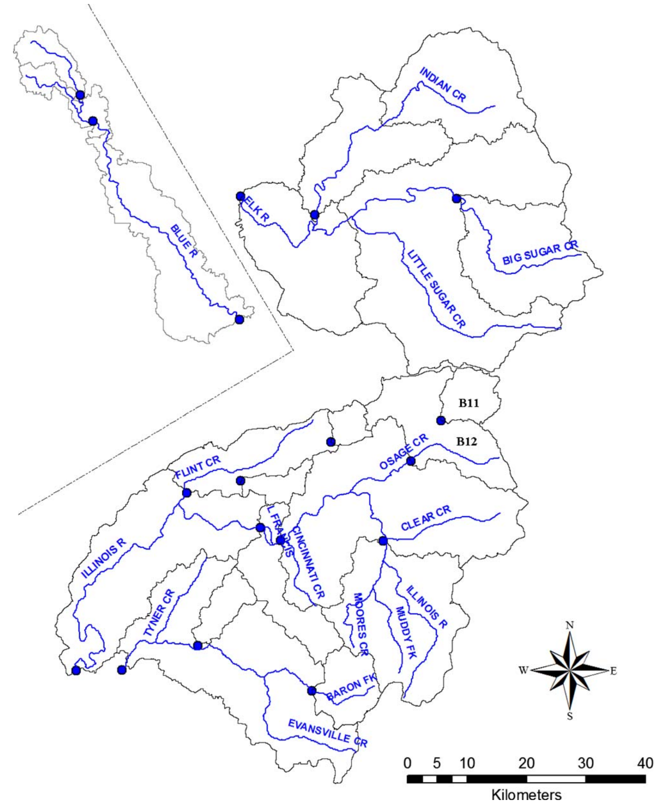

Fig. 3. Watershed delineation for DMIP Basins

delineated into five subbasins, 12 subbasins, and three subbasins corresponding to DMIP gauges for the Elk, Illinois, and Blue basins, respectively, and each of these basins is treated as a lumped area, shown in Fig. 3.

Land-Use Management and Soil Classification

Land use and soil definition are critical to determining the land use soil class combinations and distributions for each respective delineated subbasin. HSPF, in particular, needs land use and soil data to estimate the hydrologic parameters coded in the pervious (PERLND) and impervious (IMPLND) subroutines associated with land use and soil types. Spatial resolution of land use can be determined through watershed delineation processes focusing on study basins. Land use information for DMIP basins is listed in Table 1 and the soil classification map for the Illinois River Basin (the largest basin in DMIP) is shown in Fig. 4.

Table 1. Percentage of Land-Use Data for DMIP2 Basins

Land use	Elk	Illinois	Blue
Total area (km^2)	2,258	2,484	1,233
Urban or built-up land (%)	2.0	4.4	2.0
Agricultural land (%)	45.9	58.3	65.9
Forest (%)	51.8	36.7	16.0
Water (%)	0.2	0.3	16.0
Barren land (%)	0.1	0.3	0.1

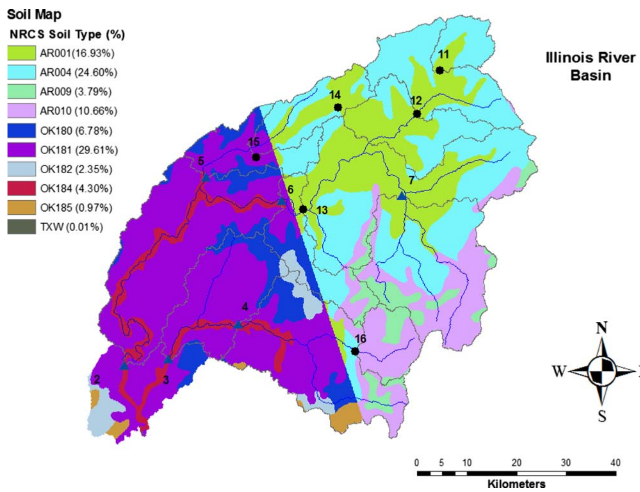

Fig. 4. Soil map for Illinois River Basin

Calibration

Parameters

The HSPF has a number of model parameters, but based on a literature review, key parameters to obtain as good a match as possible between modeled and simulated flow over the calibration period from October 1, 1996, to September 30, 2002, are listed in Table 2 (Doherty and Johnston 2003; Fontaine and Jacomino 1997; Im et al. 2003; Kim et al. 2007; Lumb et al. 1994). All these parameters are incorporated into hydrologic runoff processes associated with the PERLND module representing pervious land segments. Specific details and functions of parameters are available in a BASINS technical note (U.S. EPA 2000).

Automatic Calibration

Before PEST was available in HSPF back in 1994, manual calibration was commonly used in concert with the HSPF Expert System for Calibration (HSPEXP) (Lumb et al. 1994). Although automatic calibration using PEST is promising, a few difficulties are associated with its use in the DMIP project. First, PEST does not have the capability to compromise forcing data to calibrate annual water balance. Sometimes it is necessary to increase or decrease potential evapotranspiration to balance hydrologic input and output when the uncertainty embedded in forcing data is greater than that derived systemically from specified parameter spaces in PEST. This justification can be made by manual calibration before automatic calibration procedures. Second, PEST is prone to adopt all parameter estimates in basins, which are inherited from the characteristics of parent watersheds so that calibration should be implemented subbasin by subbasin to get more plausible results. If a watershed has more than a second-order stream network, automatic calibration is not very promising in the sense that the parameters are normally assigned to both parent and child basins with nearly the same values. However, it is still useful to estimate prospective parameters from scratch to enhance further calibration to meet specific objective functions defined by the modeler with expert knowledge. Finally, it is very challenging to calibrate watersheds in small time steps such as hourly, which is a desirable temporal unit for NWS's forecast activities. The process running time for calibration periods in the Elk River Basin, for instance, is about 20 h for a single run. However, note that this computational challenge can be overcome by using advanced computing technology, such as parallel computing, if applicable.

The search algorithm built in PEST implements a particularly robust variant of the Gauss–Marquardt–Levenberg (GML) method of parameter estimation by maintaining a continuous relationship between model parameters and model outputs (Doherty

Table 2. Initial Values and Parameter Ranges for HSPF

Parameter name	Description	Units	Initial value	Value used in literature	Range of values	
					Typical[d]	Possible[d]
AGWETP	Fraction of remaining potential evapotranspiration from active groundwater	None	0	0.05[a]	0.0–0.05	0–0.2 (1.0)
AGWRC	Base groundwater recession rate	None	0.98	0.95[a], 0.98[b], 0.99[c]	0.92–0.99	0.85 (0.001)–0.999
BASETP	Fraction of potential evapotranspiration from baseflow	None	0.02	0.1[a,b]	0.0–0.05	0–0.2 (1.0)
CEPSC	Interception storage capacity	mm	2.54	—	0.76–5.08	0.25–10.2 (25.4)
DEEPFR	Fraction of groundwater inflow to deep recharge	None	0.1	0.1[a], 0.0[b,c]	0.0–0.2	0.0–0.5 (1.0)
INFILT	Infiltration rate	mm/h	4.06	2.03[a], 1.78–15.49[b], 1.78[c]	0.25–6.35	0.025–12.7 (2540)
IRC	Interflow recession parameter	None	0.5	0.4[a], 0.6[b]	0.5–0.7	0.1–0.9
KVARY	Variable groundwater recession flow	1/mm	0	—	0.0–76.2	21.59 (0.0)–25.4
LZETP	Lower zone evapotranspiration parameter	None	0.2	0.5[a], 0.1–0.8[b], 0.5[c]	0.2–0.7	0.1–0.9 (1.5)
LSUR	Length of the assumed overland flow	m	106.7	—	60.96–152.4	30.48 (0.3)–213
LZSN	Lower zone nominal soil moisture storage	mm	152.4	—	76.2–203.2	50.8 (0.25)–381(254)
NSUR	Manning's roughness for overland flow	None	0.2	—	0.03–0.1	0.01–0.3 (1.0)
SLSUR	Slope of overland flow plane	cm/cm	0.46	—	0.30–1.52	0.03–4.57 (304.8)
UZSN	Upper zone nominal soil moisture storage	mm	28.7	12.7[a], 17.53[b], 12.7[c]	2.54–25.4	1.27–50.8 (254.0)

[a]Doherty and Johnston (2003).

[b]Kim et al. (2007).

[c]Im et al. (2003).

[d]Note that typical and possible values are from USEPA (2000), and values in parentheses are taken from the HSPF parameter section through WinHSPF graphical user interface (GUI).

Table 3. Calibration Location for DMIP2 Basins

Number	USGS ID	Name	Referred to as:	Area (km^2)	Watershed system
1	7332500	Blue River near Blue, Okla.	bluo2	1,233	Blue River
1a	7332390[c]	Blue River near Connerville, Okla.	connr	420	Blue River
2	7196500	Illinois River near Tahlequah, Okla.	talo2	2,484	Illinois River
3	7197000	Baron Fork at Eldon, Okla.	eldo2	795	Illinois River
4	7196973[b]	Peacheater Creek at Christie, Okla.	peach	65	Illinois River
5	7196000[b]	Flint Creek near Kansas, Okla.	knso2	285	Illinois River
6	7195500[b]	Illinois river near Watts, Okla.	wtto2	1,645	Illinois River
7	7194800[b]	Illinois River at Savoy, Ariz.	savoy	433	Illinois River
8	7189000	Elk River near Tiff City, Mo.	tifm7	2,258	Elk River
9	7188653[a]	Big Sugar Creek near Powell, Mo.	powel	365	Elk River
10	7188885[a]	Indian Creek near Lanagan, Mo.	lanag	619	Elk River
11	7194880[b]	Osage Creek near Cave Springs, Ark.	caves	90	Illinois River
12	7195000[b]	Osage Creek near Elm Springs, Ark.	elmsp	337	Illinois River
13	7195430[d]	Illinois River south of Siloam Springs, Ark.	sloa4	1,489	Illinois River
14	7195800[b]	Flint Creek at Springtow, Ark.	sprin	3	Illinois River
15	7195865[b]	Sager Creek near West Siloam Springs, Okla.	wsilo	49	Illinois River
16	7196900[b]	Baron Fork at Dutch Mills, Ark.	dutch	105	Illinois River

[a]Interior simulation points for Elk system.

[b]Interior simulation points for Illinois system.

[c]Interior simulation points for Blue River system.

[d]Both calibration points as basins and interior simulation points as subbasins of Illinois River system (Fig. 1).

and Johnston 2003; Marquardt 1963). Although GML, as a gradient-based method, has been criticized in the hydrology community in the sense that such a method lacks the ability to guarantee global optimum (Gupta et al. 2003), the results of numerical experiments using GML show that a GML-based method can perform well in finding the global minimum of a complex system (Skahill and Doherty 2006). Technical details and algorithms built in PEST are well documented in recent literature (Doherty and Skahill 2006; Gutierrez-Magness and McCuen 2005; Skahill and Doherty 2006).

Although the hydrologic parameters in three basins (e.g., Elk, Illinois, and Blue) are calibrated independently, the hydrologic parameters in the subbasins (e.g., five for Elk) are calibrated independently of those in the same basin so that a total of 19 subbasins (e.g., five for Elk, 12 for Illinois, and two for Blue) are delineated and calibrated. Automatic calibration was used for the majority of DMIP basin calibration runs, but a manual calibration scheme was also partially utilized in setting up initial model parameters and tuning the hydrologic model at particular peaks. Al-Abed and Whiteley (2002) pointed out that the variability of less sensitive parameters does not need to be considered during the calibration procedure, but the sensitive parameters (e.g. INFILT, LZSN, and UZSN) of HSPF in subbasins should correspond to the known physical properties of the watersheds because the values are physically interconnected with relative ranking order from the physical features within the watersheds. Sometimes, these hydrologic parameters in a single subbasin are tied to neighboring subbasins. But during automatic calibration with PEST, the tied parameters will not be calibrated separately even if such parameters will be adjusted with the same values during the calibration process if only the tied parameters are inherited from the parent watersheds. For example, in the Illinois River Basin (Fig. 1), automatic calibration was conducted subbasin by subbasin from upstream (e.g., streamflow Gauge 11 where the headwater starts) to downstream (e.g., streamflow Gauge 2 located at the mouth of the basin) via all other streamflow gauge networks (e.g., streamflow Gauges 12 and 13). Thus, as shown in Fig. 3, upstream subbasin B11, where streamflow Gauge 11 is located at the mouth of B11 and the gauge is utilized for calibration purposes, was first calibrated with PEST so that the optimal value of infiltration value, INFILT, was identified and reported as 2.54 mm/h. Next, the calibration procedures move to downstream subbasin B12, right below B11. Subbasins B11 and B12, however, are now part of the basin where streamflow Gauge 12 is utilized for calibration. In PEST, all hydrologic parameters already identified in the preceding calibration for B11 are readjusted so that the INFILT previously identified for B11 is now adjusted to 1.02 mm/h from 2.54 mm/h through the later calibration processes for B12 at streamflow Gauge 12. But the hydrologic parameters used in the previous hydrologic calibration for B11 should be maintained throughout calibration processes for B12 if those values are identified as the global minimum corresponding to objective functions in PEST during calibration processes for B11. PEST optimizes multiobjective functions tailored to B12 in this case, even if it needs to search the optimal value to guarantee the global minimum for both B11 (inner basin) and B12 (outer basin). For this reason, sometimes the hydrologic parameter must be adjusted manually to sustain the parameter already determined in the previous calibration in this context. Readjusting less sensitive hydrologic parameters during calibration would not have a significant effect on objective functions the user defined in optimization routines, but sensitive parameters, such as infiltration rate, must be taken into account to meet other statistical criteria, such as the percent absolute peak error described later. The calibration procedure used in the study area from upstream to downstream can be termed "top-down calibration" or "in-to-out calibration," but a reverse calibration procedure, such as "bottom-up calibration" or "out-to-in calibration," would also be interesting.

More detailed discussion of the advantages and disadvantages of manual and automatic calibrations is beyond the scope of this research, but some valuable information can be found in the lit-

Table 4. Calibrated Model Parameters in Major Outlets for DMIP2 Basins

Parameters (units)	Illinois River: Baron Fork at Eldon	Illinois River: South Siloam Springs	Illinois River: Tahlequah	Elk River	Blue River	All basins
	Calib.	Calib.	Calib.	Calib.	Calib.	Uncalib.
AGWETP	0.0018	0.001	0.0056	0.001	0.022	0.0
(none)	—	—	—	—	—	—
AGWRC	0.9653	0.9853	0.9969	0.959	0.9863	0.98
(none)	(−1.5%)	(0.5%)	(1.7%)	(−2.1%)	(0.6%)	—
BASETP	0.0294	0.1379	0.1554	0.0431	0.0778	0.02
(none)	(47.0%)	(589.5%)	(677.0%)	(115.5%)	(289.0%)	—
CEPSC	0.1872	0.01	0.0164	0.0179	0.3951	2.54
(mm)	(87.2%)	(−90.0%)	(−83.6%)	(−82.1%)	(295.1%)	—
DEEPFR	0.05	0.1379	0.0934	0.0167	0.0473	0.1
(none)	(−50.0%)	(37.9%)	(−6.6%)	(−83.3%)	(−52.7%)	—
INFILT	0.1084	0.0726	0.0545	0.0452	0.0761	4.1
(mm/h)	(−32.3%)	(−54.6%)	(−65.9%)	(−71.8%)	(−52.4%)	—
IRC	0.7977	0.7555	0.85	0.5864	0.6027	0.5
(none)	(59.5%)	(51.1%)	(70.0%)	(17.3%)	(20.5%)	—
KVARY (1/mm)	—	—	—	—	—	0.0
LZETP (none)	—	—	—	—	—	0.2
LSUR (m)	91.4	91.4	91.4	91.4	91.4	91.4–106.7
LZSN	50.8	50.8	50.8	82.8	53.1	165.1
(mm)	(−69.2%)	(−69.2%)	(−69.2%)	(−49.8%)	(−67.8%)	—
NSUR (none)	—	—	—	—	—	0.2
SLSUR (cm/cm)	0.82–1.85	0.46–1.30	0.46–1.46	0.45–1.40	0.44–0.46	0.046–1.85
UZSN (mm)	27.0	36.6	20.6	50.1	27.7	28.7
	(−5.8%)	(27.9%)	(−28.0%)	(74.8%)	(−3.2%)	—

Note: —=unchanged values from uncalibrated. The values in parentheses represent the percent changes of parameters in the process of calibration.

erature (Boyle et al. 2000; Chen 2003; Doherty and Johnston 2003; Kim et al. 2007). Also, the reader is referred to the literature (Doherty and Skahill 2006; Kim et al. 2007; Skahill and Doherty 2006) for details on objective functions developed for hydrologic calibration of HSPF using PEST. Table 3 represents relevant data for model calibrations, and Table 4 shows the estimated parameters used to generate streamflow for major outlets in the subbasins to evaluate model performance during calibration periods. It is noteworthy that most of the calibrated parameters for DMIP2 basins have deviated significantly from uncalibrated parameters, except for AGWRC, the groundwater base recession rate.

Results

Calibration Statistics

To evaluate the model performance of calibrated and uncalibrated simulations, statistical analysis was conducted. For statistical measures at the calibration streamflow gauges, root-mean-square error (RMSE), correlation coefficient (r), and Nash–Sutcliffe efficiency (R^2) (Nash and Sutcliffe 1970) were selected to compare the DMIP simulations to observed streamflows, and percent absolute peak error [Ep (%)] was also generated for selected individual events described in the following section. Note that an

Table 5. Calibrated and Uncalibrated Statistics during October 1, 1996–October 1, 2002, Calibration Period

	Illinois: Baron Cal	Illinois: Baron UnCal	Illinois: Siloam Cal	Illinois: Siloam UnCal	Illinois: Tahlequah Cal	Illinois: Tahlequah UnCal	Elk Cal	Elk UnCal	Blue Cal	Blue UnCal
Observed average flow (m^3/s)	10.69	10.69	18.70	18.70	30.14	30.14	22.16	22.16	10.05	10.05
Sim. average flow (m^3/s)	10.79	10.13	16.88	19.75	27.07	29.05	19.39	25.50	9.49	8.94
RMSE (%)	14.16	14.88	19.30	20.95	34.25	43.76	26.47	35.51	22.99	27.06
Correlation (r)	0.83	0.82	0.86	0.84	0.77	0.59	0.76	0.56	0.65	0.41
Nash (R^2)	0.70	0.66	0.73	0.68	0.59	0.33	0.56	0.22	0.40	0.17

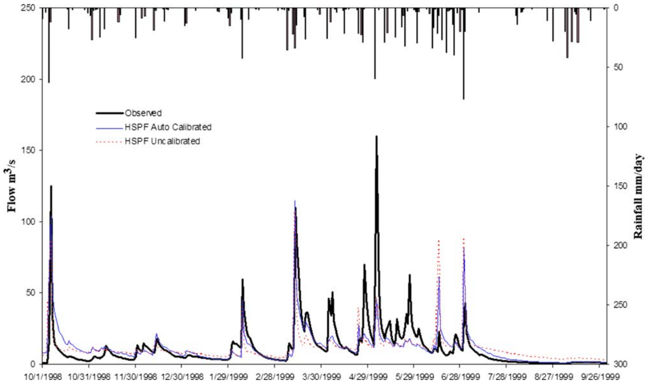

Fig. 5. Hydrograph for the Illinois River at Baron Fork for wettest water year (October 1, 1998–September 30, 1999)

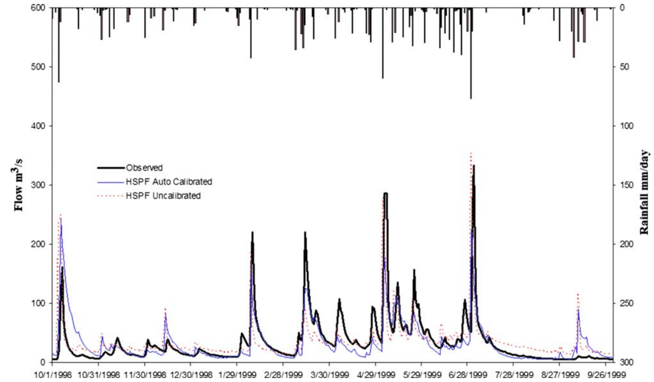

Fig. 7. Hydrograph for Illinois River at Tahlequah for wettest water year (October 1, 1998–September 30, 1999)

objective function built in PEST also takes into account statistical components, such as the summed weighted squared differences between volumes calculated on the basis of simulated and observed flows (not shown in the paper) over the entirety of the calibration and validation period (Doherty and Johnston 2003). Mathematical equations for statistical measures are available in Smith et al. (2004). As shown in Table 5, the model of calibrated simulation outperformed that of uncalibrated simulations over calibration periods. The model performances of calibration simulations at basin mouths (outlets), particularly Tahlequah, Elk, and Blue, show notable differences in statistical measures from uncalibrated simulations. Statistics in Table 5, however, reveal that calibrations of Tahlequah, Elk, and Blue watersheds are still on the poor side. This could have been averted through more rigorous manual calibration, which could be tedious and time consuming for particular peaks. Figs. 5–7 show hydrograph comparisons for the Illinois River Basin (the largest watershed in this study) in the wettest water year (October 1, 1998–September 30, 1999), to measure how the calibrated model performs against the uncalibrated model. These figures illustrate hydrograph comparisons between simulated streamflows with calibration and without calibration against observed streamflows. Overall, timing of peaks for both calibrated and uncalibrated flows match observed flows well, but the magnitude of peaks is somewhat different from observed flows at a particular location at Baron (see June 28, 1999, at Baron in Fig. 5). These magnitude differences might be explained by uncertainties related to radar overestimation of rainfall, data collection at gauge stations (Gan and Burges 2006; Sieck et al. 2007), or model parameters dealing with subsequent peak flows in that particular subbasin. However, the magnitude of peak differences on June 28, 1999, has not been seen at downstream subbasins Siloam and Tahlequah. It also appears that the calibrated simulations better represent recession flows after peak flows compared to uncalibrated flows shown in Figs. 6 and 7.

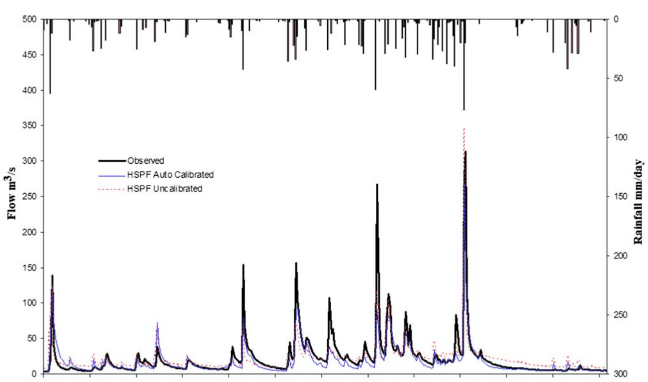

Fig. 6. Hydrograph for Illinois River at Siloam Springs for wettest water year (October 1, 1998–September 30, 1999)

Events Selected

For statistical analysis, 19 storm events (listed in Table 6) were selected for the Tahlequah Basin, which is the outlet of Illinois River Basin. Fifteen storm events are taken from a publication for the DMIP project (Reed et al. 2004), and the last four storm events were selected based on daily peaks of hydrographs corresponding to significant rainfall events (e.g., precipitation >20 mm). Note that the first 15 storm events include a wide range of event sizes, from a few small storms to the largest storms during the calibration periods, in order to identify the relationships between model structure and simulation performance over various flow ranges associated with uncalibrated and calibrated hydrologic parameters. The percent absolute peak errors for calibrated and uncalibrated simulations at Tahlequah are 60 and 150%, respectively. As one might notice, several of the uncalibrated simulations also produce relatively small errors from observed flows over selected events, including Events 1, 10, and 15. Calibrated simulations that do not achieve a small bias over uncalibrated simulations at the selected peaks tend to underestimate flows earlier in the wet season (about April–June), maintaining a small simulation bias over the whole calibration period.

Exceedance Probability of Flows

Figs. 8–10 illustrate comparisons of exceedance probability of the observed, calibrated, and uncalibrated daily flow for the Illinois River Basin over the calibration period. Exceedance probability is a good measure to evaluate how well the model simulates a wide range of streamflows, from low flows to high flows through normal flows. For instance, uncalibrated flows at Baron (Fig. 8), which is upstream of Siloam, overestimate flows against observed flows, while calibrated flows agreed very well with the observed flows. In some cases the model seems to overestimate or underestimate, but has a consistency (e.g., underestimating high flows and overestimating low flows), as shown in Figs. 9 and 10. Simulated flows with calibration, however, are in fairly good agreement but are underestimated for high flows in all subbasins in the Illinois River. In low-flow situations, in particular, simulated flow

Table 6. Selected Events for Tahlequah

	Periods (hrs)				Peak (m^3/s)		
Event	Start		End		Obs.	Uncal.	Cal.
1	May 10, 1996	1600	May 17, 1996	1300	262	202	80
2	November 4, 1996	1200	November 14, 1996	2300	498	917	245
3	November 24, 1996	0100	December 5, 1996	0900	483	1,670	834
4	February 19, 1997	0200	February 25, 1997	2300	597	1,380	303
5	August 17, 1997	0000	August 23, 1997	2300	42	83	89
6	January 4, 1998	0000	January 16, 1998	2300	729	1,290	331
7	March 16, 1998	0000	March 26, 1998	2300	349	110	109
8	October 5, 1998	0000	October 11, 1998	2300	206	983	270
9	February 7, 1999	0000	February 15, 1999	2300	276	420	233
10	April 4, 1999	0000	April 10, 1999	2300	132	72	54
11	May 4, 1999	0000	May 11, 1999	2300	370	1,950	219
12	June 24, 1999	0000	July 6, 1999	2300	556	1,650	820
13	January 2, 2000	0000	January 9, 2000	2300	40	44	36
14	May 26, 2000	0000	June 1, 2000	2300	191	2,940	626
15	June 15, 2000	1300	June 21, 2000	1200	483	324	216
16	February 22, 2001	0000	March 4, 2001	2300	718	1,180	290
17	December 16, 2001	0000	December 21, 2001	2300	557	114	168
18	April 8, 2002	0000	April 12, 2002	2300	561	155	126
19	August 15, 2002	0000	August 16, 2002	2300	211	190	233

gain showed much improvement through calibration, and it is anticipated that HSPF would be a suitable model for drought studies associated with low flows.

Conclusion and Future Work

The HSPF model is used to simulate streamflows for the DMIP project. Geographic Information System (GIS) capabilities and enriched geospatial databases enable the HSPF model to derive parameters from physical watershed properties, including land-use management, digital elevation, and soil profiles. The measures of model performance are presented in terms of summaries of statistics over calibration periods. Hydrologic simulations without calibration are also evaluated to assess how well initial hydrologic parameters can be captured based on physical hydrologic processes associated with watershed delineation. Overall, calibrated simulations outperformed uncalibrated simulations in terms of statistical measures, including RMSE, correlation coefficient, Nash–Sutcliffe efficiency, and percent absolute peak error.

The automatic calibration software PEST, which is a model-independent-parameter estimator, is used for this study, and it shows reasonably well estimated initial hydrologic parameters derived from physical watershed configuration. Although automatic calibration using PEST performed well in HSPF, the writer anticipates that additional enhancements and improvement are required for PEST to be fully applicable to complex watershed calibration efforts. The current version of PEST remains difficult to calibrate because of a lack of physical significance in calibration processes in PEST (Whittemore 2004). It is possible that physical significance can be distorted within the optimization routine, where objective function is optimized forcibly depending on modelers' specified objectives. Physical parameters should be clearly defined in constraint sets and linked to runoff equations and other physically based subroutines to obtain feasible solutions

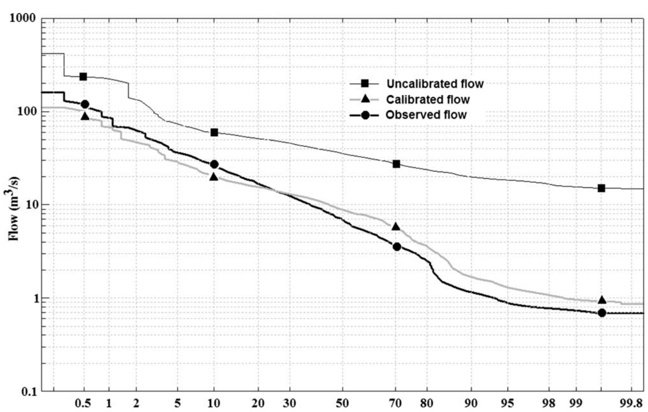

Fig. 8. Exeedance probability of observed and simulated flow with/without calibration over calibration period at Baron

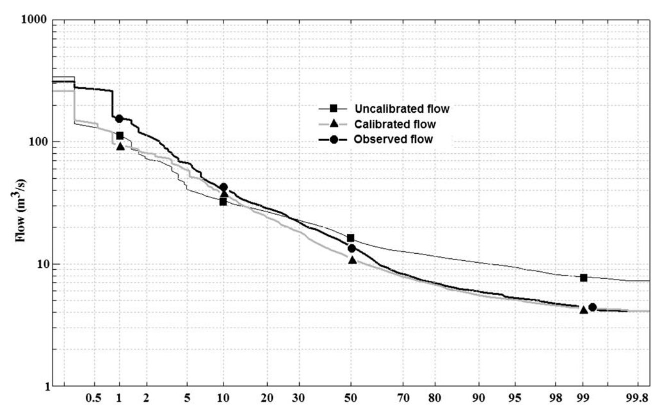

Fig. 9. Exeedance probability of observed and simulated flow with/without calibration over calibration period at Siloam

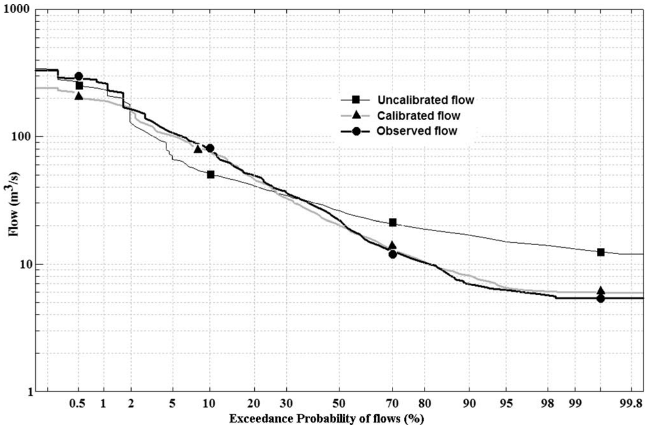

Fig. 10. Exeedance probability of observed and simulated flow with/without calibration over calibration period at Tahlequah

in a multiobjective optimization framework. Another aspect of calibration in this context with PEST is the relationship of hydrologic parameters between prior and posterior calibration for multiple subbasins within same-parent watersheds. For instance, although hydrologic parameters are determined through preceding calibration processes for inner subbasins, the parameters are readjusted through latter calibration processes for outer subbasins. If calibrated simulation for an outer subbasin requires parameter adjustment for an inner subbasin, the hydrologic parameter within the inner subbasin is always compromised to optimize the objective function established for the outer subbasin even if the optimal parameters in the inner subbasin are already identified in the previous calibration. To overcome these drawbacks embedded in PEST associated with basin networks and identification of feasible parameter sets during calibration processes, either a "top-down calibration" or "bottom-up calibration" scheme suited with more rigorous optimization routines, such as genetic algorithms and neural networks, would be good options to optimize multiobjective functions embedded in calibration building blocks. Particularly, a genetic algorithm, which mimics nature's evolution mechanisms, is more suitable for complex systems like the study basins in the sense that it finds a local minimum much more effectively than traditional methods (e.g., gradient-base approaches) that require good starting values for the parameters involved and high nonlinearity convergence to an optimal solution. Also, a genetic algorithm guarantees to find a global optimum only if it exits. Additionally, although a genetic algorithm has capabilities of sensitivity analysis through parameter uncertainty and shadow prices, which represent the rate of change of parameters contributing to the measure of performance for multiobjective functions, rigorous sensitivity analysis of key hydrologic parameters using a Monte Carlo simulation framework would also be beneficial to examine the modeled flows for errors associated with the parameters and rainfall input.

Another aspect of PEST in the context of sensitivity analysis is statistical interference between parameters within parameter sets. Parameters are often estimated independently so that there is no joint effect associated with physically based dependent parameters such as infiltration rate, Manning roughness, hydraulic conductivity, and soil characteristics on simulation result (Chen 2003). To explore which variables have the most impacts on model results, model-wide uncertainty analysis is an important topic and will be considered in future research. The basic variables may include model coefficients, parameters, boundary conditions, input variables, and other factors that are considered in the model. Having obtained estimates of all the main effects and interaction effects within variable sets, the most sensitive parameters in the model can be ruled out. Such efforts will provide useful insights to improve calibration techniques in aid of either manual calibration with HSPEXP or autocalibration with PEST.

Finally, although the writer presumed that the radar data used in this study have been rigorously quality controlled by NWS/NOAA, it should be noted that in many cases, the storm total is compared to one or at most a few ground rain gauges, all of which have storm undercatch. In the literature, the *Z-R* relationship varies through a storm, when typically a single *Z-R* is used (Austin 1987; Steiner et al. 1999). As Steiner et al. (1999) notes, evaluating HSPF performances as inputs of different size of the spatial domain in rainfall distribution would be interesting future research to investigate how much difference there is between the radar rainfall estimates at gauge locations and the sampling volume resolution differences between radar and gauge versus the natural variability of rainfall. The answers to these questions will add the momentum to build a case toward the use of NEXRAD data over sparsely or possibly ungauged watersheds.

Acknowledgments

The writer thanks five anonymous reviewers for insightful comments and suggestions, which helped improve the quality of the manuscript substantially.

References

Al-Abed, N. A., and Whiteley, H. R. (2002). "Calibration of the hydrological simulation program Fortran (HSPF) model using automatic calibration and geographical information systems." *Hydrolog. Process.*, 16(16), 3169–3188.

Anderson, J. R., Hardy, E. E., Roach, J. T., and Witmer, R. E. (1976). "A land use and land cover classification system for use with remote sensor data." *Geological Survey Professional Paper 964*, U.S. Geological Survey, U.S. Dept. of the Interior, Reston, Va.

Austin, P. M. (1987). "Relation between measured radar reflectivity and surface rainfall." *Mon. Weather Rev.*, 115(5), 1053–1070.

Bell, V. A., and Moore, R. J. (1998). "A grid-based distributed flood forecasting model for use with weather radar data. Part 2: Case studies." *Hydrology Earth Syst. Sci.*, 2(3), 283–298.

Boyle, D. P., Gupta, H. V., and Sorooshian, S. (2000). "Toward improved calibration of hydrologic models: Combining the strengths of manual and automatic methods." *Water Resour. Res.*, 36(12), 3663–3674.

Boyle, D. P., Gupta, H. V., and Sorooshian, S. (2001). "Toward improved streamflow forecasts: Value of semidistributed modeling." *Water Resour. Res.*, 37(11), 2749–2759.

Carpenter, T. M., and Georgakakos, K. P. (2004). "Impacts of parametric and radar rainfall uncertainty on the ensemble streamflow simulations of a distributed hydrologic model." *J. Hydrol.*, 298(1–4), 202–221.

Chen, C. W. (2003). "Discussion of 'Methodologies for calibration and predictive analysis of a watershed model' by John Doherty and John M. Johnston." *J. Am. Water Resour. Assoc.*, 39(6), 1561–1562.

Doherty, J., and Johnston, J. M. (2003). "Methodologies for calibration and predictive analysis of a watershed model." *J. Am. Water Resour. Assoc.*, 39(2), 251–265.

Doherty, J., and Skahill, B. E. (2006). "An advanced regularization methodology for use in watershed model calibration." *J. Hydrol.*, 327, 564–577.

Ek, M. B., et al. (2003). "Implementation of Noah land surface model advances in the National Centers for Environmental Prediction operational mesoscale eta model." *J. Geophys. Res.*, 108(D22), 8851.

Fontaine, T. A., and Jacomino, V. M. F. (1997). "Sensitivity analysis of simulated contaminated sediment transport." *J. Am. Water Resour. Assoc.*, 33(2), 313–326.

Fulton, R. A., Breidenbach, J. P., Seo, D.-J., and Miller, D. A. (1998). "The WSR-88d rainfall algorithm." *Weather Forecast.*, 13(2), 377–395.

Gan, T. Y., and Burges, S. J. (2006). "Assessment of soil-based and calibrated parameters of the Sacramento model and parameter transferability." *J. Hydrol.*, 320, 117–131.

Greene, D. R., and Hudlow, M. D. (1982). "Hydrometeorologic grid mapping procedures." *Proc., AWRA Int. Symp. on Hydrometeorology*, Denver, Colo., A. I. Johnson and R. A. Clark, eds., AWRA, Bethesda, Md.

Gupta, H. V., Sorooshian, S., Hogue, T. S., and Boyle, D. P. (2003). "Advances in automatic calibration of watershed models." *Water Science and Application Series*, Q. Duan, S. Sorooshian, H. V. Gupta, A. N. Rousseau, and R. Turcotte, eds., Vol. 6, American Geophysical Union, 197–211.

Gutierrez-Magness, A., and McCuen, R. H. (2005). "Effect of flow proportions on HSPF model calibration accuracy." *J. Hydrol. Eng.*, 10(5), 343–352.

Im, S., Brannan, K. M., and Mostaghimi, S. (2003). "Simulating hydrologic and water quality impacts in an urbanizing watershed." *J. Am. Water Resour. Assoc.*, 39(6), 1465–1479.

Kim, S. M., Benham, B. L., Brannan, K. M., Zeckoski, R. W., and Doherty, J. (2007). "Comparison of hydrologic calibration of HSPF using automatic and manual methods." *Water Resour. Res.*, 43, W01402.

Koren, V. I., Finnerty, B. D., Schaake, J. C., Smith, M. B., Seo, D.-J., and Duan, Q. Y. (1999). "Scale dependencies of hydrology models to spatial variability of precipitation." *J. Hydrol.*, 217, 285–302.

Lumb, A. M., McCammon, R. B., and Kittle, J. L., Jr. (1994). "Users manual for an expert system (HSPEXP) for calibration of the hydrologic simulation program—FORTRAN." *U.S. Geological Survey Water-Resources Investigations Rep. No. 94–4168*, Reston, Va.

Marquardt, D. W. (1963). "An algorithm for least-squares estimation of nonlinear parameters." *J. Soc. Ind. Appl. Math.*, 11(2), 431–441.

Mesinger, F., et al. (2004). "NCEP North American regional reanalysis." *Proc., 15th Symp. on Global Change and Climate Variations*, American Meteorological Society, Boston.

Michaud, J., and Sorooshian, S. (1994). "Comparison of simple versus complex distributed runoff models on a midsized semiarid watershed." *Water Resour. Res.*, 30(3), 593–605.

Mitchell, K., et al. (2004). "NCEP completes 25-year North American reanalysis: Precipitation assimilation and land surface are two hallmarks." *GEWEX News*, 14(2), 9–12.

Nash, J. E., and Sutcliffe, J. V. (1970). "River flow forecasting through conceptual models: Part I—A discussion of principles." *J. Hydrol.*, 10(3), 282–290.

Ogden, F. L., and Julien, P. Y. (1994). "Runoff model sensitivity to radar rainfall resolution." *J. Hydrol.*, 158, 1–8.

Reed, S. M., et al. (2004). "Overall distributed model intercomparison project results." *J. Hydrol.*, 298, 27–60.

Refsgaard, J. C., and Knudsen, J. (1996). "Operational validation and intercomparison of different types of hydrological models." *Water Resour. Res.*, 32(7), 2189–2202.

Shah, S. M., O'Connell, P. E., and Hosking, J. R. M. (1996a). "Modeling the effects of spatial variability in rainfall on catchment response. 1: Formulation and calibration of a stochastic rainfall field model." *J. Hydrol.*, 175, 66–88.

Shah, S. M., O'Connell, P. E., and Hosking, J. R. M. (1996b). "Modeling the effects of spatial variability in rainfall on catchment response. 2: Experiments with distributed and lumped models." *J. Hydrol.*, 175, 89–111.

Sieck, L. C., Burges, S. J., and Steiner, M. (2007). "Challenges in obtaining reliable measurements of point rainfall." *Water Resour. Res.*, 43, W01420.

Skahill, B. E., and Doherty, J. (2006). "Efficient accommodation of local minima in watershed model calibration." *J. Hydrol.*, 329, 122–139.

Smith, M. B., et al. (2004). "The distributed model intercomparison project (DMIP): Motivation and experiment design." *J. Hydrol.*, 298, 4–26.

Steiner, M., Smith, J. A., Burges, S. J., Alonso, C. V., and Darden, R. W. (1999). "Effect of bias adjustment and rain gauge data quality control on radar rainfall estimation." *Water Resour. Res.*, 35(8), 2487–2503.

United States Department of Agriculture (USDA). (1994). "State soil data use information." U.S. Soil Conservation Service, Department of Agriculture, Washington, D.C., ⟨http://www.ftw.nrcs.usda.gov/stst_data.html⟩ (February 1, 2007).

U.S. Environmental Protection Agency (EPA). (2000). "BASINS technical note 6: Estimating hydrology and hydraulic parameters for HSPF." *EPA-823-R-00-012*, Office of Water, Washington, D.C.

Vieux, B. E., Gui, Z., and Gaur, A. (2004). "Evaluation of a physics-based distributed hydrologic model for flood forecasting." *J. Hydrol.*, 298, 155–177

Wang, D., Smith, M. B., Zhang, Z., Reed, S. M., and Koren, V. I. (2000). "Statistical comparison of mean areal precipitation estimates from WSR-88d, operational and historical gage networks." *Proc., 15th Conf. on Hydrology*, American Meteorological Society, Long Beach, Calif.

Whittemore, R. C. (2004). "Discussion: Methodologies for calibration and predictive analysis of a watershed model by John Doherty and John M. Johnston." *J. Am. Water Resour. Assoc.*, 40(1), 267.

Wilson, C. B., Valdes, J. B., and Rodriquez-Iturbe, I. (1979). "On the influence of the spatial distribution of rainfall on storm runoff." *Water Resour. Res.*, 15(2), 321–328.

Young, C. B., Bradley, A. A., Krajewski, W. F., and Anton, K. (2000). "Evaluating NEXRAD multisensor precipitation estimates for operational hydrologic forecasting." *J. Hydrometeorol.*, 1(3), 241–254.